Study On The Effect of Bond Strength On The Failure Mode of Coarse-Grained Sandstone In Weakly Cemented Stratum

Xianda Yang
JiangXi University of Science and Technology https://orcid.org/0000-0001-9334-9436
Lihui Sun (834428026@qq.com)
https://orcid.org/0000-0002-2207-2609
Jiale Song
Hebei University of Engineering
Bensheng Yang
Hebei University of Engineering
Chengren Lan
Hebei University of Engineering

Research

Keywords: weakly cemented stratum, bond strength, failure mode, ground control, parallel bond model

Posted Date: August 31st, 2021

DOI: https://doi.org/10.21203/rs.3.rs-818844/v1

Version of Record: A version of this preprint was published at Minerals on December 31st, 2021. See the published version at https://doi.org/10.3390/min12010055.

Abstract

Bond strength is one of the most important parameters and can affect the macroscopic mechanical properties and the damage state of the rock to some degree. The coarse-grained sandstone with strength of less than 40 MPa was studied by the controlled variable method. The influence of parallel bond strength on the peak strength and failure mode of coarse-grained sandstone was simulated, the evolution law of peak strength and failure mode of bond strength were comprehensively analyzed. The results show that the peak strength of rock was positively correlated with the bond strength, the difference value between tensile and shear crack was negatively correlated with tensile bond strength and positively correlated with shear bond strength. Tensile-shear bond strength ratio less than 0.5, the peak strength of the rock was usually stable at the certain extreme value under a constant tensile bond strength. Tensile crack was negatively correlated with the tensile-shear bond strength ratio, shear crack was positively correlated with the tensile-shear bond strength ratio. The failure mode of coarse-grained sandstone is shear failure. The research results can be used to guide the ground control of other mine stopes or roadways with weak cementation lithology.

Introduction

Weakly cemented coal measures are widespread in western China (Zhang et al., 2015, Meng et al., 2016). However, its diagenesis environment in Western China was different from that in central and eastern China (Wang et al., 2019,). The insufficient diagenesis results in the low strength, easy disintegration, easy weathering, poor cementation of the weakly cemented rock; once exposed to water, the weakly cemented rock tend to be muddy (Meng et al., 2015, Bai et al., 2020). As a result, the failure, rupture, and fracture of the surrounding rock under the mining disturbance in the western mining area are different from that in the central-eastern mining area (Yang et al., 2017, Zhang et al., 2018). When the macroscopic cracks of weakly cemented rock are not through, the rock can be considered as an entirety. When the collapse failure occurs, the rock becomes a loose mass, which has a great relationship with the cementation performance of the rock. Bond strength is an important index to characterize the performance of rock cementation. The mechanical properties and failure mode of weakly cemented rocks can be further explored by studying the relationship between bond strength and rock strength.

The particle flow discrete element method has been widely used to study microscopic mechanical properties of the rock. In the PFC program software, the particle flow discrete element method is used as the basis for the theory, the rigid bodies with masses are used as particles, and the interaction motion and force action between particles are studied to solve the macroscopic and complex practical problems (Shimizu et al., 2010). At present, the relationship between micro-parameters and macro-mechanical properties of rocks had been studied by PFC software (Potyondy and Cundall, 2004, Hsieh et al., 2008, Kazerani and Zhao, 2010, Su et al., 2011, Yi et al., 2011, Zhou et al., 2012, Obermayr et al, 2013, Zhang et al., 2016, Zhang et al, 2019, Wang Min, 2020). ABi analyzed the quantitative relationship between micro-parameters and the macro-parameters by means of variable control, and the results of the laboratory tests were consistent with those of the numerical simulation, indicating that micro-parameter results are

reliable (ABi et al., 2018). Cong analyzed the correlation between the macroscopic mechanical characteristics of the rock and the microscopic parameters through the loading and unloading tests on the marble. The elastic modulus of the parallel bond was linearly related to the macroscopic elastic modulus; in particular, the secondary failure surface of the rock sample decreases with the increase of the friction factor (Cong et al., 2015). Zhao discussed the influence of some microscopic parameters of the parallel bonding model on the macroscopic deformation parameters (Zhao et al., 2012). Su analyzed the effect of particle size on macro-mechanical properties by uniaxial compression simulation tests (Su et al., 2018). Through different experimental design methods, Yoon obtained microscopic parameters that have a significant influence on the failure characteristics of the model (Yoon J, 2007). By numerical experiments, Yang fitted the approximate expressions of the compressive strength, elastic modulus, and Poisson's ratio of the parallel bonding model (Yang et al., 2006). Xu developed a fine-scale structural model of limestone and obtained the microscopic parameters mechanical parameters of limestone (Xu et al., 2011). Through uniaxial compression and Brazilian splitting tests, Deng concluded that the peak strength of hard rocks was mainly influenced by the bond strength (Deng et al., 2019). In previous studies, the relationship between macroscopic mechanical properties and micro-parameters of rocks was discussed from different perspectives. It was pointed out that microscopic parameters determine the mechanical behavior characteristics of rocks. Hard rocks were mainly studied in these studies, while soft rocks have been rarely discussed. In western China mines, the rock strength of most coal seams is relatively low, and the surrounding rock of roadways is subject to frequent deformation. It is of guiding significance for roadway support to deeply study the influence of the weakly cemented rocks (Wang et al., 2017, Meng et al., 2014).

Considering the real conditions of weakly cemented rocks in western mining areas, the influence of the bond strength on the peak strength and the failure mode of rock were investigated through numerical simulation. This paper provides a basis and reference for further understanding of the relationship between the strength of weakly cemented rocks and the development of cracks in surrounding rocks after engineering disturbances.

Models

2.1 Basic mechanical parameters of coarse-grained sandstone

Hongqinghe Coal Mine is located in the southwest of Erdos City, Inner Mongolia Autonomous Region, China. Coal seams in this mine are a typical weakly cemented formation, with low rock strength and easy disintegration once exposed to water. During the roadway excavation of Hongqinghe Coal Mine, coarse-grained sandstone samples were collected and processed into standard test pieces of Φ50mm100mm according to the method recommended by the international society of rock mechanics. Table 1 shows the basic mechanical properties of weakly cemented coarse-grained sandstone after laboratory tests.

Table 1
Basic mechanical parameters of coarse-grained sandstone

Parameter	Specimen 1	Specimen 2	Specimen 3	Specimen 4	Specimen 5	Specimen 6
Compressive strength /MPa	11.56	27.25	13.52	15.37	22.35	30.16
Tensile strength /MPa	1.30	2.87	0.85	0.74	1.88	2.98
Cohesion /MPa	3.30	6.53	3.30	3.30	6.53	6.53
Internal friction angle /°	35.20	39.10	35.20	35.20	39.10	39.10

2.2 Discrete element model of coarse-grained sandstone

The research has shown that the parallel bond model discrete element particle model can be used to simulate many kinds of mechanical properties of rock-like materials (Yoon J, 2007). The tensile bond strength and shear bond strength in the parallel bond model had a great influence on the change of peak strength and the evolution of failure mode.

The research results of previous scholars were generally the study of multiple micro-parameters on macro-parameters, and there were few studies on the macroscopic properties of rock by a single parameter. This article only studies the influence of bond strength (tensile bond strength and shear bond strength) on rock failure.

Based on the basic mechanical properties of weakly cemented coarse-grained sandstone in Hongqinghe Coal Mine, the rock with peak strength of less than 40 MPa was used for analysis. According to the basic mechanical data of coarse-grained sandstone in Hongqinghe Coal Mine and the parameter of previous research (Su et al., 2018), the micro parameters of the parallel bond model were determined (Table 2), and the two-dimensional granular flow coarse-grained sandstone model was constructed, in which tensile bond strength and shear bond strength were only the two influencing parameters. Since coarse-grained sandstone with peak strength less than 40 MPa was used, the upper limits of tensile bond strength and shear bond strength were considered. For simplicity, it was assumed that the same values of tensile bond strength and shear bond strength were the maximum values of the peak strength of the coarse-grained sandstone model within the numerical range. As shown in Fig. 1.

Table 2
Micro-parameters of the model

Parameter	Value	Parameter	Value	Parameter	Value
Particle density/ $kg{\cdot}m^{-3}$	2195	Particle stiffness ratio	2.6	PBM stiffness ratio	2.6
Porosity	0.16	PBM elastic modulus /Pa	4e9	PBM Radius factor	1.0
Particle size ratio	1.66	Local damping coefficient	0.7	Particle friction coefficient	0.6

If $\overline{\sigma}_c = \overline{\tau}_c$ = 27 MPa and σ_u = 40 MPa, then the bond strength ranged from 1 ~ 27 MPa. When the value of the bond strength was the integer, the number of experimental results was $C_{27}^1 C_{27}^1$ = 729, which was a large amount of data. If the value of the bond strength was taken as an integral multiple of 5, the number of experimental results was $C_6^1 C_6^1 = 36$, which was difficult to characterize the macro parameter law of rock. For the above reasons, the integral multiple of 2 was selected as the value of the bond strength, and the total number of experimental results was $C_{14}^1 C_{14}^1$ = 196.

Experimental Results And Analysis

3.1 Relationship between bond strength and peak strength

Figure 2a shows the effect of tensile bond strength on peak strength. When the shear bond strength was 1 MPa, the change of the tensile bond strength had little effect on the peak strength. When the shear bond strength was 3–17 MPa, the growth rate of the curve decreased when the two bond strength were equal. When the shear bond strength was 19–27 MPa, the relationship between peak strength and tensile bond strength had a linearly increased relationship as follows.

Figure 2b shows the effect of shear bond strength on peak strength. It can be seen that when the tensile bond strength was 1–13 MPa, the peak strength increased rapidly at first and then increased slowly; when the upper limit of peak strength was reached, it no longer increased. However, when the tensile bond strength was 13–27 MPa, there was no upper limit of the peak strength.

Through the comparison of Fig. 2a and Fig. 2b, it can be seen that the relationship between peak strength and tensile bond strength was positively correlated, the relationship between peak strength and shear bond strength was positively correlated. But the influence of tensile bond strength and shear bond strength on peak strength was different. Through the comparison, the relationship between peak strength and shear bond strength can be divided into three stages: if shear bond strength ranged from 1–7 MPa, peak strength was in the accelerated increase stage; if shear bond strength ranged from 9–17 MPa, peak strength was in the slow increase stage; and if shear bond strength ranged from 19–27 MPa, peak strength was in the stable fluctuation stage. The relationship between peak strength and shear bond

strength also experienced a three-stage change, which was more convergent than that between peak strength and shear bond strength. Besides, if the tensile bond strength or shear bond strength increased, the value of peak strength did not change from the curve of tensile bond strength or shear bond strength of 1 MPa. Because the rock formations mined in western mines are mostly weakly cemented rock formations, the rock strength is generally low, and the tensile bond strength is more accurate than the shear bond strength for the rock strength adjustment. The focus of research can be on the influence of the tensile bond strength on other low-strength weakly cemented rocks.

3.2 Effect of bond strength on failure mode

Under uniaxial compression, tensile and shear cracks were generated on the rock by tensile and shear bond fractured caused by stress. If there were more tensile cracks than shear cracks, the failure mode was the tensile failure; otherwise, it was the shear failure. In this paper, the failure mode was characterized by the difference between tensile crack and shear crack. If the difference between tensile crack and shear crack was positive, the failure mode was the tensile failure. If the difference between tensile crack and shear crack was negative, the failure mode was the shear failure. If the difference between tensile crack and shear crack was zero, the failure mode was the composite tensile-shear failure.

Figure 3a shows the effect of tensile bond strength on the difference between tensile crack and shear crack. It can be seen that there was a negative correlation between tensile bond strength and the difference between tensile crack and shear crack. When the shear bond strength was 1 MPa, the difference between tensile crack and shear crack rapidly decreased from positive value to negative value and then tended to be stable. When the shear bond strength was 3–13 MPa, the difference between tensile crack and shear crack decreased slowly from positive value to negative value. When the shear bond strength was 15–27 MPa, the difference between tensile crack and shear crack was positive.

Figure 3b shows the effect of tensile bond strength on the difference between tensile crack and shear crack. It can be seen that there was a positive correlation between the difference between tensile crack and shear crack and tensile bond strength. When the tensile bond strength was 1 MPa, the difference between tensile crack and shear crack was positive. When the tensile bond strength was 3–27 MPa, the difference between tensile crack and shear crack increased rapidly at first, then increased slowly, and then gradually increased from negative value to positive value.

When the tensile bond strength increased, the shear bond was broken before the tensile bond, and then shear cracks were generated. In other words, as shown in Fig. 3a, with the increase of tensile bond strength, the difference between tensile crack and shear crack decreased and more shear cracks are generated and less the difference between tensile crack and shear crack, and the failure mode of rock was transferred from tensile failure into shear failure. When the shear bond strength increased, the tensile bond was broken before the shear bond, and tensile cracks were generated. As shown in Fig. 3b, with the increase of shear bond strength, more tensile cracks were generated, the difference between tensile crack and shear crack increased, and failure mode of rock was changed from shear failure to tensile failure. Studying the failure modes of weakly cemented rocks is the prerequisite for exploring the failure laws of

the rock formations in western mining areas. The control strength of the rock formations is an important guarantee for the safe production of the mine. Further research on the failure modes of the rocks is needed.

3.3 Effect of tensile-shear bond strength ratio

In this section, the influence of tensile-shear bond strength ratio on peak strength of rock can be accurately characterized. Figure 4 shows the effect of tensile-shear bond strength ratio on peak strength. When the shear bond strength was 1–7 MPa, the peak strength increased to the maximum value, and the increase of the tensile-shear bond strength ratio had little effect on the peak strength. Combining Fig. 3, it can be seen that the peak strength had maximum value in the same two bond strengths. As shown in Fig. 4, the rock with shear bond strength of more than 7 MPa also had the maximum value.

Figure 5 shows the effect of tensile-shear bond strength ratio on the difference value between tensile crack and shear crack. When the tensile-shear bond strength ratio was less than 2, the difference value between tensile crack and shear crack was more than 0, and tensile failure occurred in the rock. When the tensile-shear bond strength ratio was more than 2, the difference value between tensile crack and shear crack was less than 0, and shear failure occurred in the rock. When the tensile-shear bond strength ratio was 2, the difference value between tensile crack and shear crack was 0, and the composite tensile-shear failure occurred in the rock.

Discussion

4.1 Analysis of maximum value of peak strength

As shown in Fig. 4, the hypothesis was not true that the peak strength was the maximum value when the tensile-shear bond strength ratio was 1. Therefore, the relationship between tensile-shear bond strength ratio and peak strength should be further discussed.

Since the assumption was not valid, the law obtained in Fig. 4 was considered, the integer of the tensile-shear bond strength ratio within 1–10 was taken. First, the shear bond strength remained unchanged, the tensile-shear bond strength ratio was taken as an integer within 1–10. Second, the tensile bond strength was unchanged and the tensile-shear bond strength ratio was taken as the value, the peak strength decreased gradually and the maximum value of the peak strength not can be judged. Therefore, the tensile bond strength was unchanged and the value of tensile bond strength was based on the inverse of tensile-shear bond strength ratio K_c^{-1} (the shear-tensile bond strength ratio), as shown in Fig. 6.

Figure 6a shows that when the tensile-shear bond strength ratio was 7, the peak strength with different shear bond strength was the maximum value of the peak strength. Figure 6b shows that when the inverse of tensile-shear bond strength ratio was 2, i.e. the tensile-shear bond strength ratio was 0.5, the peak strength was the maximum value. When the tensile-shear bond strength ratio was less than 0.5, the peak strength was the maximum value and no longer increased with the increase of shear bond strength.

Therefore, when the tensile bond strength was constant, the tensile-shear bond strength ratio less than 0.5 should be avoided when the shear bond strength was increased.

According to the data fitting in Fig. 6a, the functional relationship between the tensile-shear bond strength ratio and shear bond strength, and the functional relationship between the maximum value of the peak strength and shear bond strength of rock was obtained as follows:

$K_c = 7$ (1)

$$\sigma_m = -0.23252 + 3.10425\ \bar{\tau}_c - 0.00477\ \bar{\tau}_c^2 \quad (2)$$

where K_c is the tensile-shear bond strength ratio; σ_m is the maximum value of the peak strength; $\bar{\tau}_c$ is the shear bond strength.

According to the data fitting in Fig. 6b, the functional relationship between the inverse of tensile-shear bond strength ratio and tensile bond strength, and the functional relationship between the maximum value of the peak strength and tensile bond strength of rock was obtained.

$$K_c^{-1} = 2 \quad (3)$$

$$\sigma_m = 1.28799 + 1.44852\ \bar{\sigma}_c + 0.01121\ \bar{\sigma}_c^2 \quad (4)$$

where K_c^{-1} is the inverse of tensile-shear bond strength ratio; $\bar{\sigma}_c$ is the tensile bond strength.

When the tensile bond strength or the shear bond strength was set, the maximum value of the peak strength and the tensile-shear bond strength ratio can be calculated. In Fig. 7a, the shear bond strength was 13 MPa and the tensile-shear bond strength ratio was7; in Fig. 7b, the tensile bond strength was 23 MPa and the inverse of tensile-shear bond strength ratio was 2, i.e. the tensile-shear bond strength ratio was 0.5, the peak strength was 40 MPa. The function slope of the maximum value of the peak strength and tensile bond strength was smaller than that of the maximum value of the peak strength and shear bond strength. The change of tensile bond strength had a more delicate influence on the maximum value of the peak strength. Therefore, the tensile bond strength was more effective than the shear bond strength in controlling the peak strength of the rock. The strength of the rock can be adjusted within the range of greater than 0.5 and less than 7 by adjusting the tensile-shear bond strength ratio, and according to the law of the extreme value of the peak strength of the rock, combined with the in-situ stress, the corresponding support and support methods can be adjusted.

4.2 Analysis of failure mode limit and crack evolution

Because when the tensile-shear bond strength ratio was 2, the difference value between tensile crack and shear crack was 0, and the failure mode of rock was more complex. In this section, when the tensile-shear bond strength ratio was near 2 (K_c = 1.8, 1.9, 2.0, 2.1, 2.2), the situation of the difference value between tensile crack and shear crack was discussed. Because the tensile bond strength was negatively correlated

with the tensile-shear bond strength ratio, the experimental data were arranged according to the same shear bond strength.

Figure 8 shows the relationship between the difference value between tensile crack and shear crack and tensile-shear bond strength ratio. When the shear bond strength was 19 MPa, the peak strength was 42.4 MPa, which was beyond the scope of the study, and the test data would not be added. It can be seen that when the difference value between tensile crack and shear crack was 0, the tensile-shear bond strength ratio was concentrated on 1.9–2.0; therefore, the limit of tensile failure and shear failure was 1.9–2.0, and the failure mode of rock was the composite tensile-shear failure. Combined with the data in Fig. 5, it was concluded that (1) the failure mode of rock was the tensile failure if tensile-shear bond strength ratio was less than 1.9; (2) the composite tensile-shear failure if tensile-shear bond strength ratio was 1.9–2.0; (3) the shear failure if tensile-shear bond strength ratio was more than 2.0.

Figure 9 shows the comparison of failure modes on tensile-shear bond strength ratio. Shear crack was green, tensile crack was yellow. It can be clearly seen that the evolution rule of tensile cracks and shear cracks with the increase of tensile-shear bond strength ratio. The bond strength was relatively low, the cracks generated by bond fracture were distributed all over the rock interior, and then the cracks gathered together to form the failure zone (tensile failure or shear failure). With the increase of the tensile-shear bond strength ratio, the shear crack increased gradually, and the tensile cracks decreased gradually. The failure mode was changed from the tensile failure of multiple fracture zones in the middle of the rock to the shear failure in the direction of a single diagonal fracture zone.

4.3 Failure mode of coarse sandstone

The rock sample used in the test was weakly cemented coarse-grained sandstone in Hongqinghe Coal Mine. The core was cut according to the international rock mechanics test standard, and the SAS-2000 servo testing machine was used to perform this test. Figure 10 show the stress-strain evolution curve and crack evolution process of the laboratory test and numerical simulation. The stress-strain curves of the laboratory test and numerical test were approximately the same, and there were some differences between the growth rate of the elastic stage and the decline rate of the post-peak stage. The local difference in the evolution of the stress-strain curve was explained as follows: there were original micro-cracks in the coarse-grained sandstone samples, while there were no micro-cracks in the numerical simulation model. According to the crack evolution rule in Fig. 10 and failure results of the laboratory tests, it can be seen that the crack is firstly generated from the ends of rock, which affected the peak strength of the coarse-grained sandstone. In the middle section of the post-peak stage, the main cracks of the failure mode of the coarse-grained sandstone were basically formed. The failure mode of coarse-grained sandstone was the shear failure, and the crack of coarse-grained sandstone in the numerical simulation was mainly shear crack (green crack). The failure mode of coarse-grained sandstone in the numerical simulation was also consistent with that of coarse-grained sandstone in the laboratory test. The peak strength and elastic modulus of numerical simulation and laboratory test were the same, the evolution rule of stress-strain curve was consistent, and the failure crack was the same.

According to the experiment and the study of the influence of bond strength on rock properties, it is concluded that the strength of the weakly cemented coarse-grained rock formation in Hongqinghe Coal Mine is about 20 Mpa and the rock formation is characterized by shear failure, combined with the law of mine pressure in the western mines. Targeted control is carried out according to the characteristics of rock formation, and the research results of this paper are instructive for the control of mine rock formations.

Conclusion

By simulating different parameters of bond strength of weakly cemented coarse-grained sandstone, the influence of bond strength on peak strength and failure mode was determined. The mechanical parameters and failure crack of weakly cemented coarse-grained sandstone were verified by laboratory tests. The following conclusions are drawn:

(1) In the numerical simulation of the bond strength of weakly cemented coarse-grained sandstone, the tensile bond strength is more sensitive to changes in the peak strength and failure mode of weakly cemented coarse-grained sandstone than the shear bond strength. When other weakly cemented rocks are studied, the tensile bond strength should be emphasized.

(2) Tensile bond strength and shear bond strength are established separately as a function of peak strength. When the tensile-shear bond strength ratio ranges from 0.5 to 7, the peak strength of weakly cemented coarse-grained sandstone can vary with the change of bond strength. When the tensile-shear bond strength ratio is out of this range, the peak strength will not change. Therefore, the tensile-shear bond strength ratio should be emphasized in studying weakly cemented rocks.

(3) When the tensile-shear bond strength ratio is greater than 2.0, the failure mode of the rock is the shear failure. When the bond strength ratio is less than 1.9, the failure mode of the rock is the tensile failure. When the bond strength ratio is 1.9–2.0, the failure mode of the rock is tensile-shear composite failure. The failure mode of weakly cemented coarse-grained sandstone is the shear failure, and the bond strength ratio is more than 2.0.

(4) Through the detection and experiment of rock samples, according to the strength and fracture mode of the reference rock, the precursor traces of the rock formation fracture in the stope can be identified, and the rock formation can be controlled in time to prevent major fracture damage. This research has guiding significance for control of mine rock formation.

Declarations

Funding

This research is financially supported by the National Natural Science Foundation of China (grant No. 52074100, grant No. 51874113); the Key Research and Development Plan Project of Hebei

province (grant No. 19275508D); the Key Laboratory of Mine Geological Disaster Mechanism and Prevention and Control (grant No. KF2018-07).

Ethical standards

The experiments comply with the current laws of the country.

Conflict of interest

The authors declare that they have no conflict of interest.

Availability of data and material

Not applicable.

Code availability

Not applicable.

Authors' contributions

Not applicable.

Ethics approval

Not applicable.

Consent to participate

Not applicable.

Consent for publication

Not applicable.

References

1. Abi ED, Zheng YR, Feng XT, Cong Y (2018) Relationship between particle micro and macro mechanical parameters of parallel-bond model. Rock Soil Mechanics 39:1289–1301. https://doi.org/10.16285/j.rsm.2016.0900
2. Bai Y, Shan RL, Ju Y, Wu YX, Sun PF, Wang ZE (2020) Study on the mechanical properties and damage constitutive model of frozen weakly cemented red sandstone. Cold Reg Sci Technol 171:102980. https://doi.org/10.1016/j.coldregions.2019.102980
3. Cong Y, Wang ZQ, Zheng YR, Feng XT (2015) Experimental study on microscopic parameters of brittle materials based on particle flow theory. Chinese Journal of Geotechnical Engineering

37:1031–1040. https://doi.org/10.11779/CJGE201506009

4. Deng SX, Zheng YL, Feng LP, Zhu PY, Ni Y (2019) Application of Design of Experiments in Microscopic Parameter Calibration for Hard Rocks of PFC3D Model. Chinese Journal of Geotechnical Engineering 41:655–664. https://doi.org/10.11779/CJGE201904008
5. Hsieh YM, Li HH, Huang TH, Jeng FS (2008) Interpreta-tions on how the macroscopic mechanical behavior of sand-stone affected by microscopic properties—Revealed by bonded-particle model. Eng Geol 99:1–10. https://doi.org/10.1016/j.enggeo.2008.01.017
6. Kazerani T, Zhao J (2010) Micromechanical parameters in bonded particle method for modeling of brittle material failure. Int J Numer Anal Methods Geomech 34:1877–1895. https://doi.org/10.1002/nag.884
7. Meng QB, Han LJ, Qiao WG, Lin DG, Fan JD (2014) Support technology for mine roadways in extreme weakly cemented strata and its application. International Journal of Mining Science Technology 24:157–164. https://doi.org/10.1016/j.ijmst.2014.01.003
8. Meng QB, Han LJ, Sun JW, Min FQ, Feng W, Zhou X (2015) Experimental study on the bolt–cable combined supporting technology for the extraction roadways in weakly cemented strata. International Journal of Mining Science Technology 25:113–119. https://doi.org/10.1016/j.ijmst.2014.11.010
9. Meng QB, Han LJ, Xiao Y, Li H, Wen SY, Zhang J (2016) Numerical simulation study of the failure evolution process and failure mode of surrounding rock in deep soft rock roadways. International Journal of Mining Science Technology 26:209–221. https://doi.org/10.1016/j.ijmst.2015.12.006
10. Obermayr M, Dressler K, Vrettos C, Eberhard P (2013) A bonded-particle model for cemented sand. Comput Geotech 49:299–313. https://doi.org/10.1016/j.compgeo.2012.09.001
11. Potyondy DO, Cundall PA (2004) A bonded-particle model for rock. International Journal of Rock Mechanics Mining Sciences 41:1329–1364. https://doi.org/10.1016/j.ijrmms.2004.09.011
12. Shimizu H, Murata S, Ishida T (2010) Effects of particle number and size distribution on macroscopic mechanical properties of rock models in DEM. Journal of the Society of Materials Science Japan 59:219–226. https://doi.org/10.2472/jsms.59.219
13. Su H, Dang CH, LI YJ (2011) Study of numerical simulation of acoustic emission in rock of inhomogeneity. Rock Soil Mechanics 32:1886–1890. https://doi.org/10.16285/j.rsm.2011.06.025
14. Su H, Yang JQ, Hu BW, Gao X, Ma H (2018) Study of particle size effect of rock model based on particle discrete element method. Rock Soil Mechanics 39:4642–4650. https://doi.org/10.16285/j.rsm.2017.0945
15. Wang Q, Pan R, Jiang B, Li SC, He MC, Sun HB, Wang L, Qin Q, Yu HC, Luan YC (2017) Study on failure mechanism of roadway with soft rock in deep coal mine and confined concrete support system. Eng Fail Anal 81:155–177. https://doi.org/10.1016/j.engfailanal.2017.08.003
16. Wang ZK, Li WP, Wang QQ, Liu SL, Hu YB, Fan KF (2019) Relationships between the petrographic, physical and mechanical characteristics of sedimentary rocks in Jurassic weakly cemented strata. Environ Earth Sci 78:131. https://doi.org/10.1007/s12665-019-8130-6

17. Wang M (2020) A scale-invariant bonded particle model for simulating large deformation and failure of continua. Comput Geotech 126:103735. https://doi.org/10.1016/j.compgeo.2020.103735
18. Xu JM, Xie ZL, Jia HT (2011) Simulation of mesomechanical properties of limestone using particle flow code. Rock Soil Mechanics 30:2084–2089. https://doi.org/10.16285/j.rsm.2010.s2.039
19. Yang BD, Jiao Y, Lei ST (2006) A study on the effects of microparameters on macroproperties for specimens created by bonded particles. Eng Comput 23:607–631. https://doi.org/10.1108/02644400610680333
20. Yoon J (2007) Application of experimental design and optimization to PFC model calibration in uniaxial compression simulation. Int J Rock Mech Min Sci 44:871–889. https://doi.org/10.1016/j.ijrmms.2007.01.004
21. Yi CW, Liang B, Jiang LG (2011) Analysis of relationship between macro-micro-parameters of sandy soil based on particle flow theory. Journal of China Coal Society 36:264–267. https://doi.org/10.13225/j.cnki.jccs.2011.s2.019
22. Yang SQ, Chen M, Jing HW, Chen KF, Meng B (2017) A case study on large deformation failure mechanism of deep soft rock roadway in Xin'An coal mine, China. Eng Geol 217:89–101. https://doi.org/10.1016/j.enggeo.2016.12.012
23. Zhao GY, Dai B, Ma C (2012) Study of effects of microparameters on macroproperties for parallel bonded model. Chin J Rock Mechan Eng 31:1491–1498. https://doi.org/10.3969/j.issn.1000-6915.2012.07.024
24. Zhou B, Wang HB, Zhao WF, Li JW, Zheng BC (2012) Analysis of relationship between particle mesoscopic and macroscopic mechanical parameters of cohesive materials. Rock Soil Mechanics 33:3171–3175. https://doi.org/10.16285/j.rsm.2012.10.019
25. Zhang JH, Wang LG, Li QH, Zhu SS (2015) Plastic zone analysis and support optimization of shallow roadway with weakly cemented soft strata. International Journal of Mining Science Technology 25:395–400. https://doi.org/10.1016/j.ijmst.2015.03.011
26. Zhang XP, Jang YJ, Wang G, Wang JC, Wu XZ, Zhang YZ (2016) Numerical experiments on rate-dependent behaviors of granite based on particle discrete element model. Rock Soil Mechanics 37:2679–2686. https://doi.org/10.16285/j.rsm.2016.09.033
27. Zhang JP, Liu LM, Cao JZ, Yan X, Zhang FT (2018) Mechanism and application of concrete-filled steel tubular support in deep and high stress roadway. Constr Build Mater 186:233–246. https://doi.org/10.1016/j.conbuildmat.2018.07.118
28. Zhang SH, Wu SC, Duan K (2019) Study on the deformation and strength characteristics of hard rock under true triaxial stress state using bonded-particle model. Comput Geotech 112:1–16. https://doi.org/10.1016/j.compgeo.2019.04.005

Figures

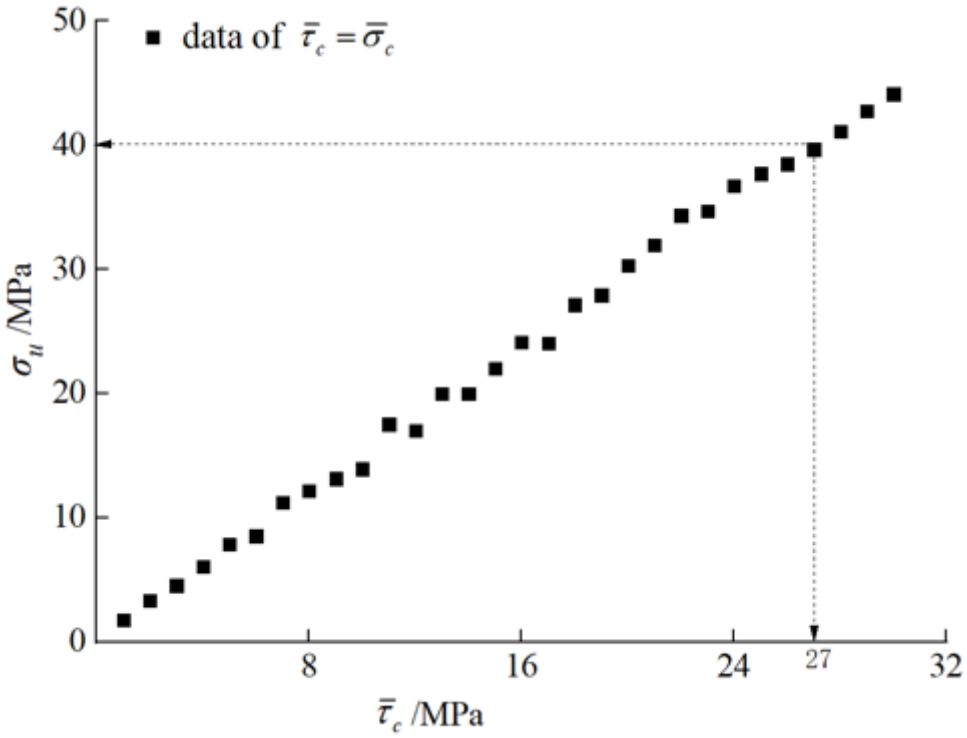

Figure 1

The relationship between the equivalence bond strength and peak strength

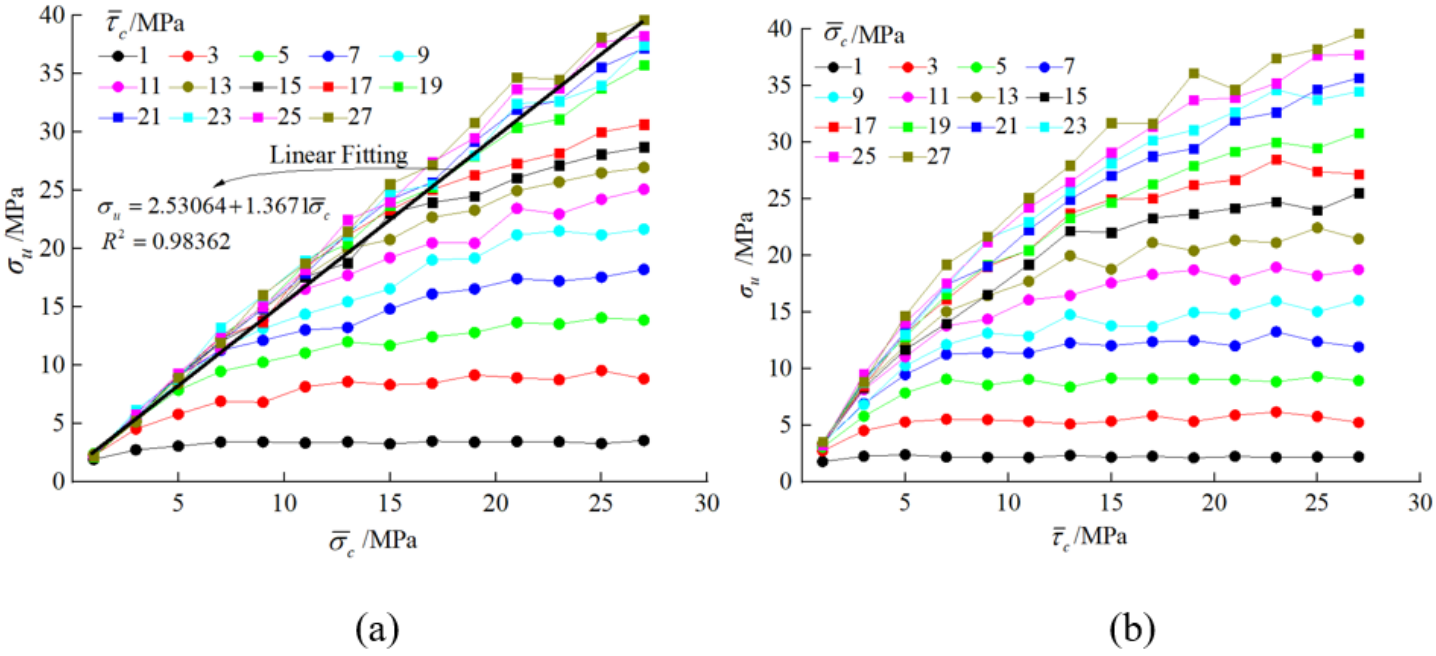

Figure 2

Effects of bond strength on peak strength; (a) tensile bond strength; (b) shear bond strength

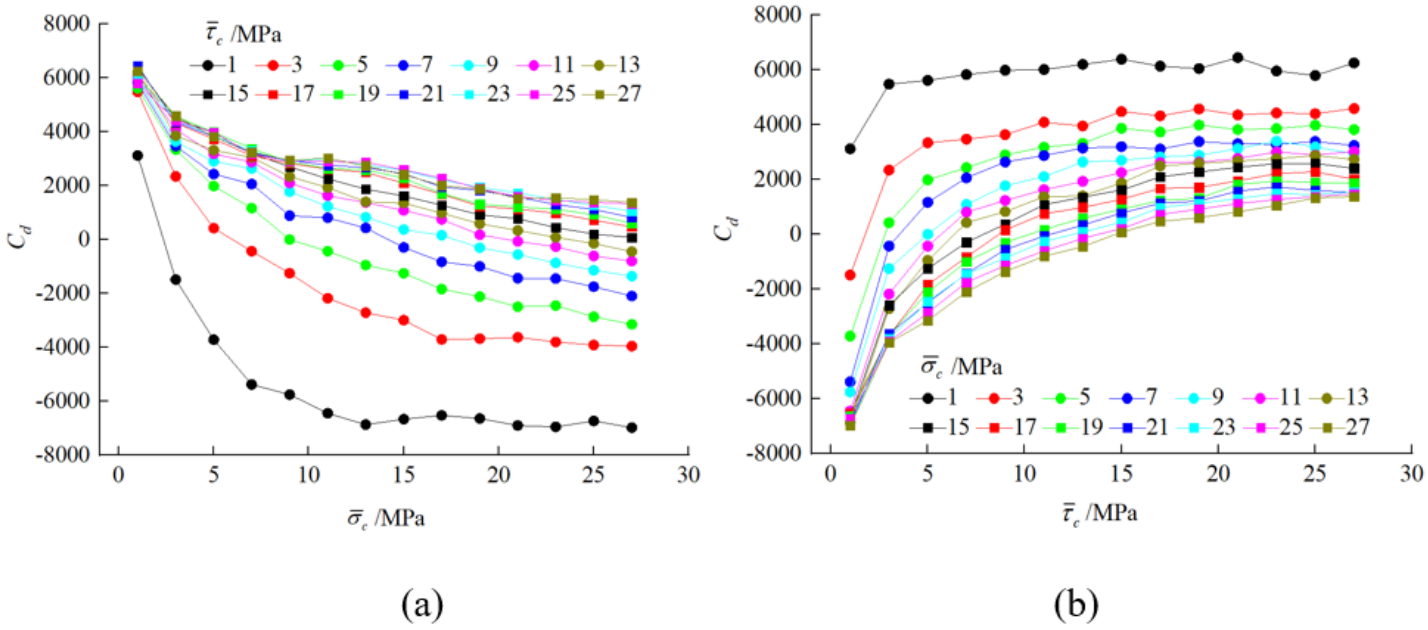

Figure 3

Effects of bond strength on the difference between tensile crack and shear crack; (a) tensile bond strength; (b) shear bond strength

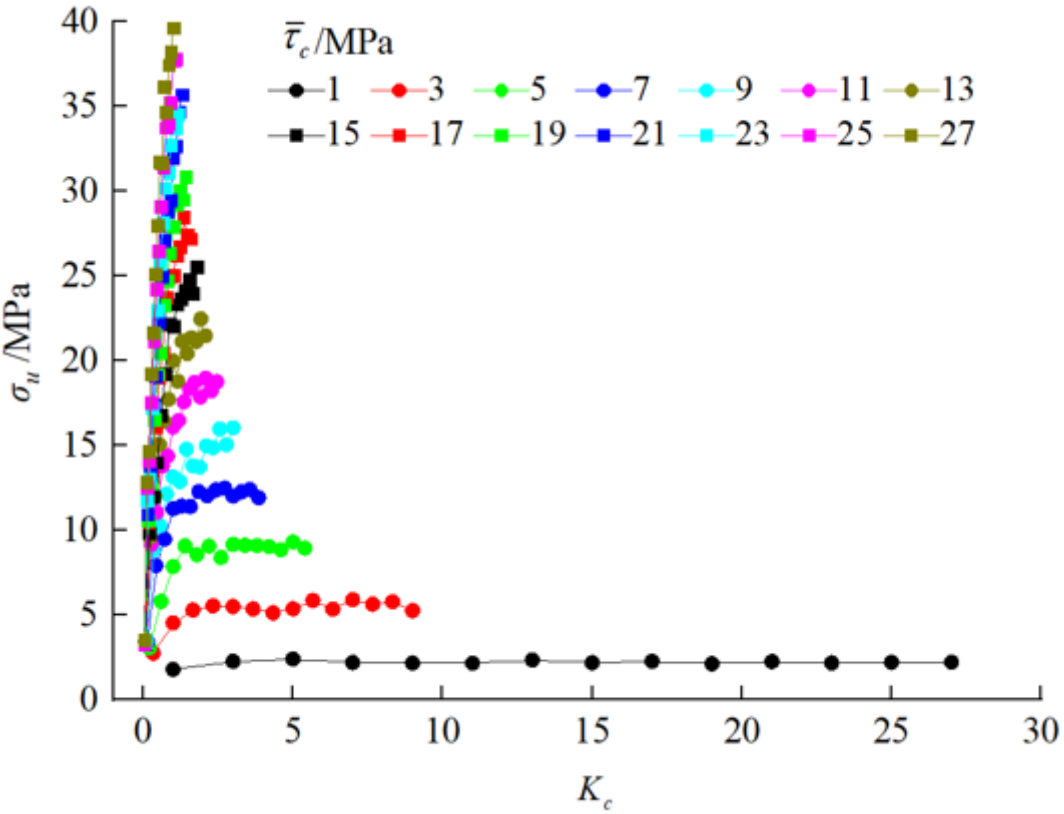

Figure 4

Effects of tensile-shear bond strength ratio on peak strength

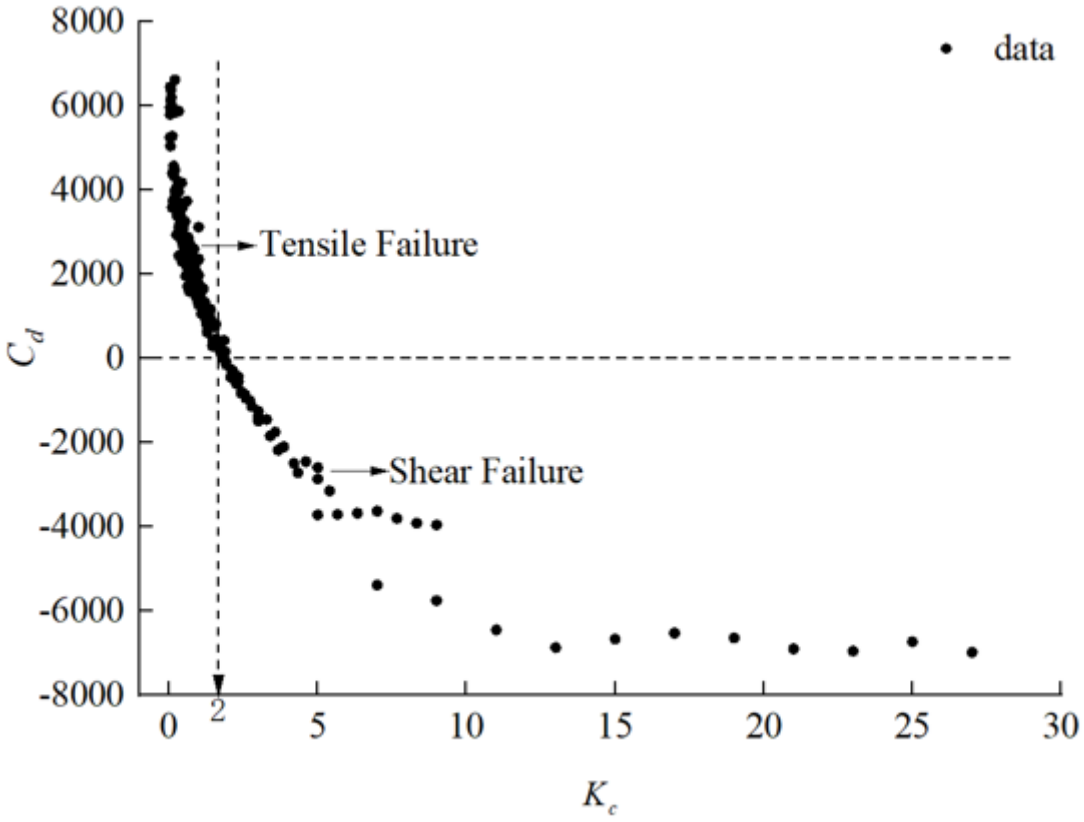

Figure 5

Effects of tensile-shear bond strength ratio on the difference between tensile and shear crack

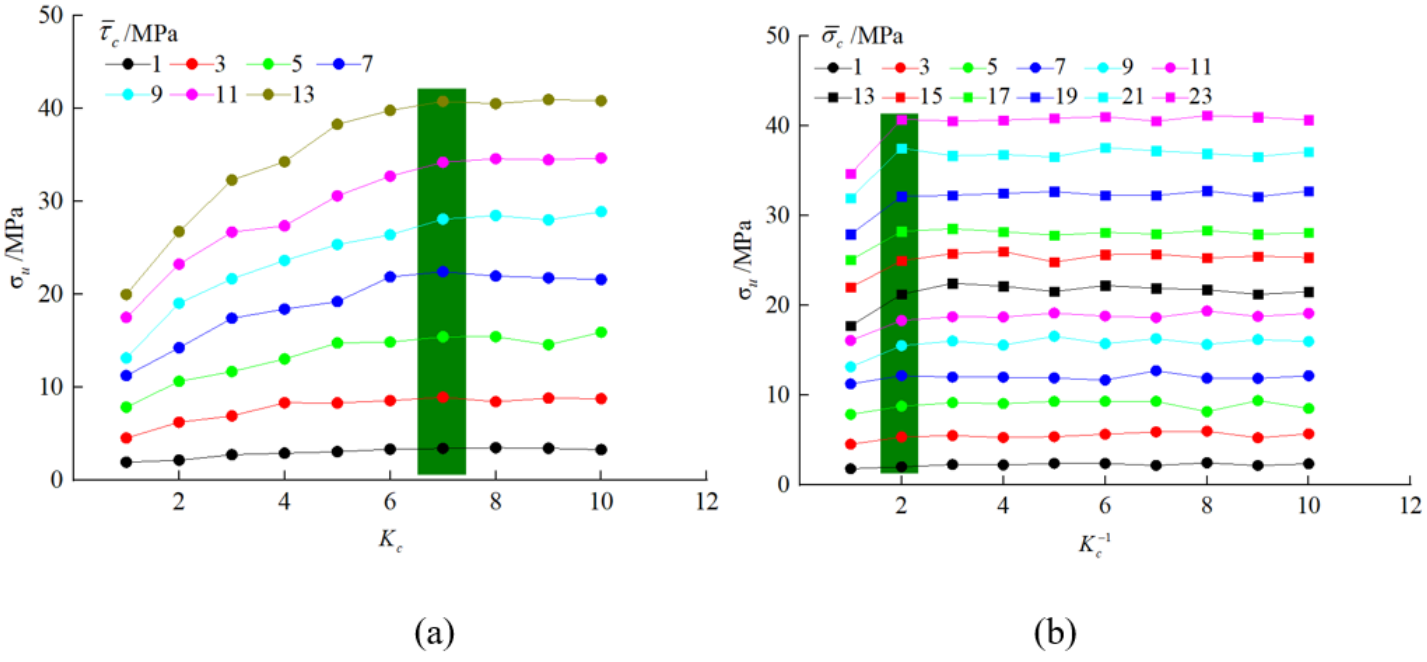

Figure 6

Effects of the bond strength ratio on peak strength; (a) tensile-shear bond strength ratio; (b) shear-tensile bond strength ratio

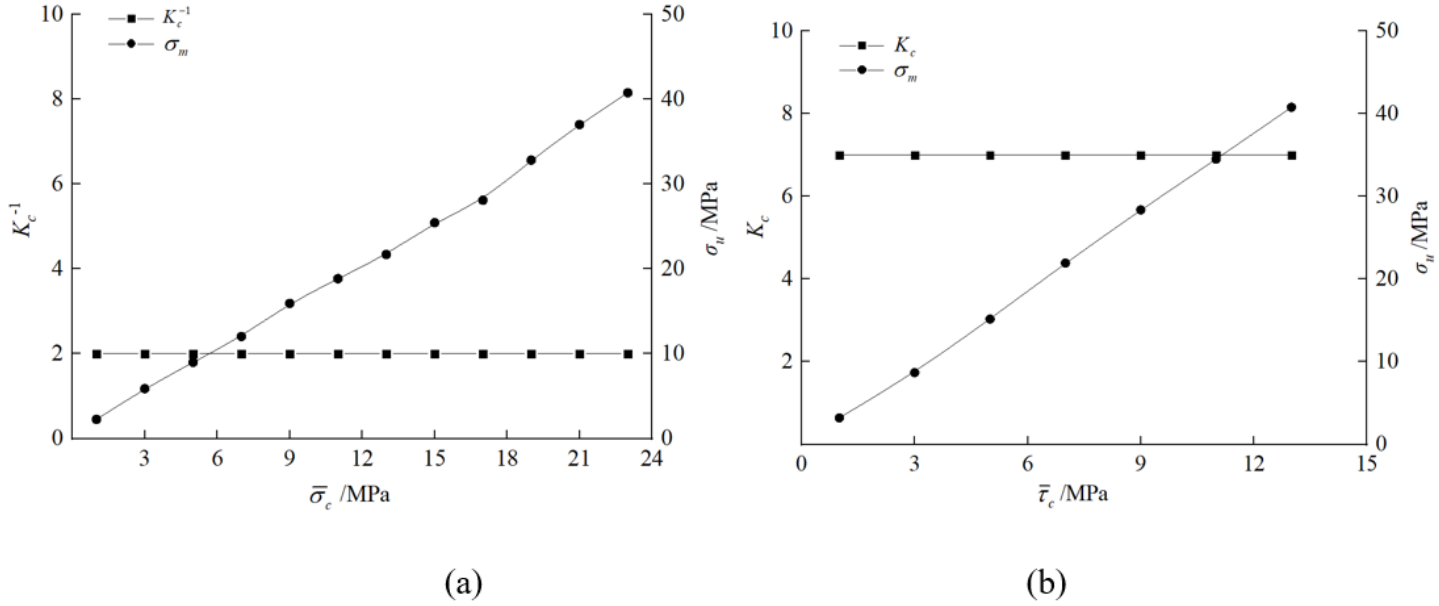

Figure 7

The relationship between bond strength and the maximum value of the peak strength; (a) tensile bond strength; (b) shear bond strength

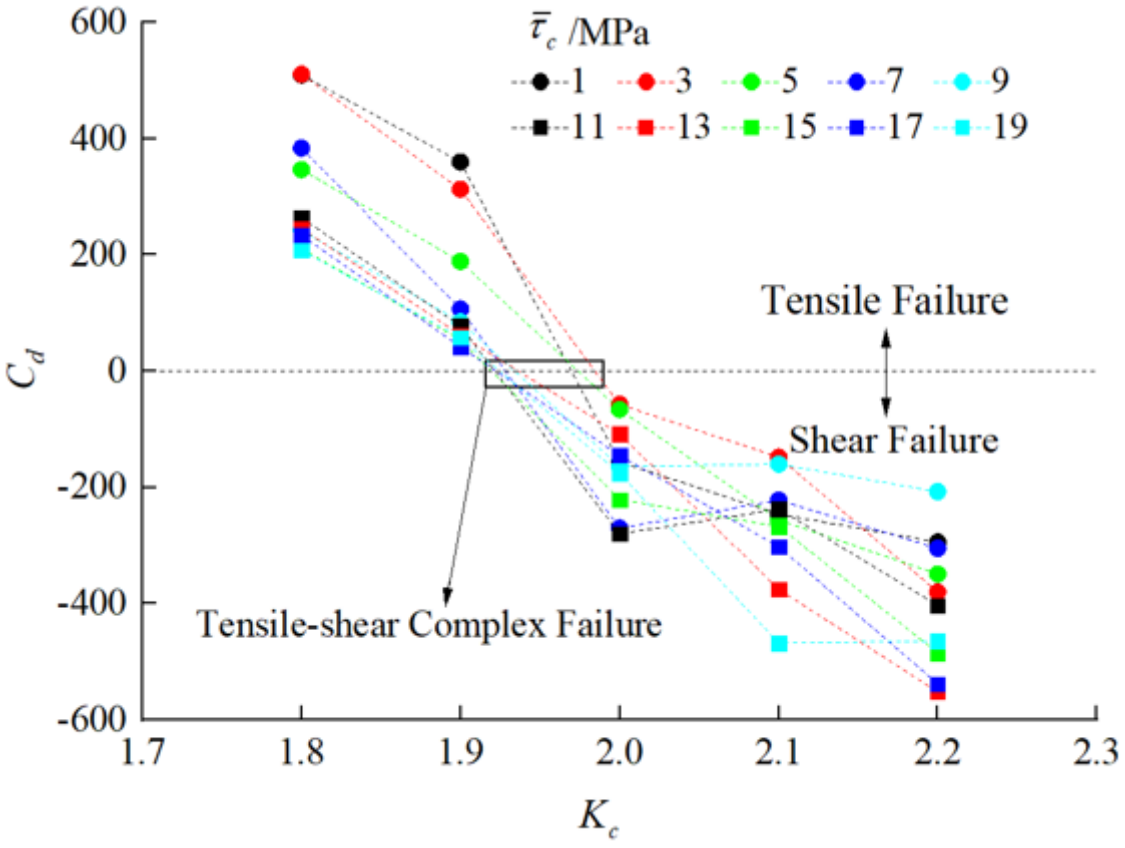

Figure 8

Effects of tensile-shear bond strength ratio on the difference between tensile and shear crack

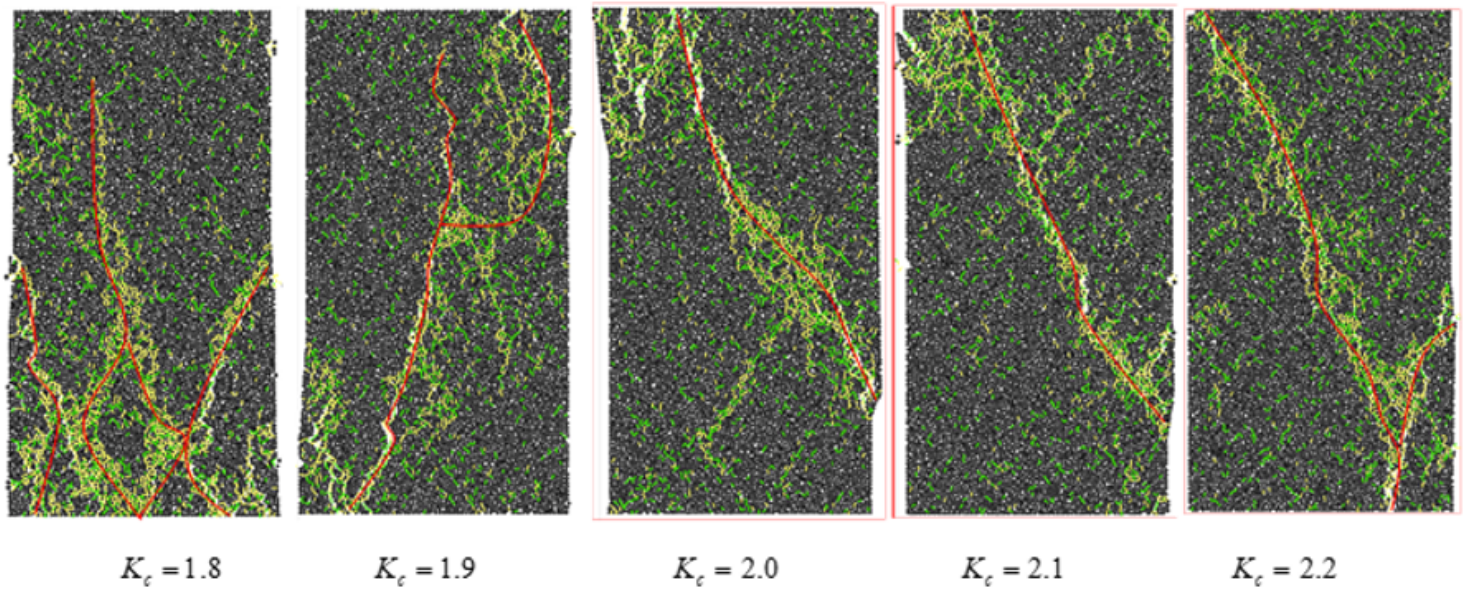

Figure 9

Failure mode of rock with different tensile-shear bond strength ratio

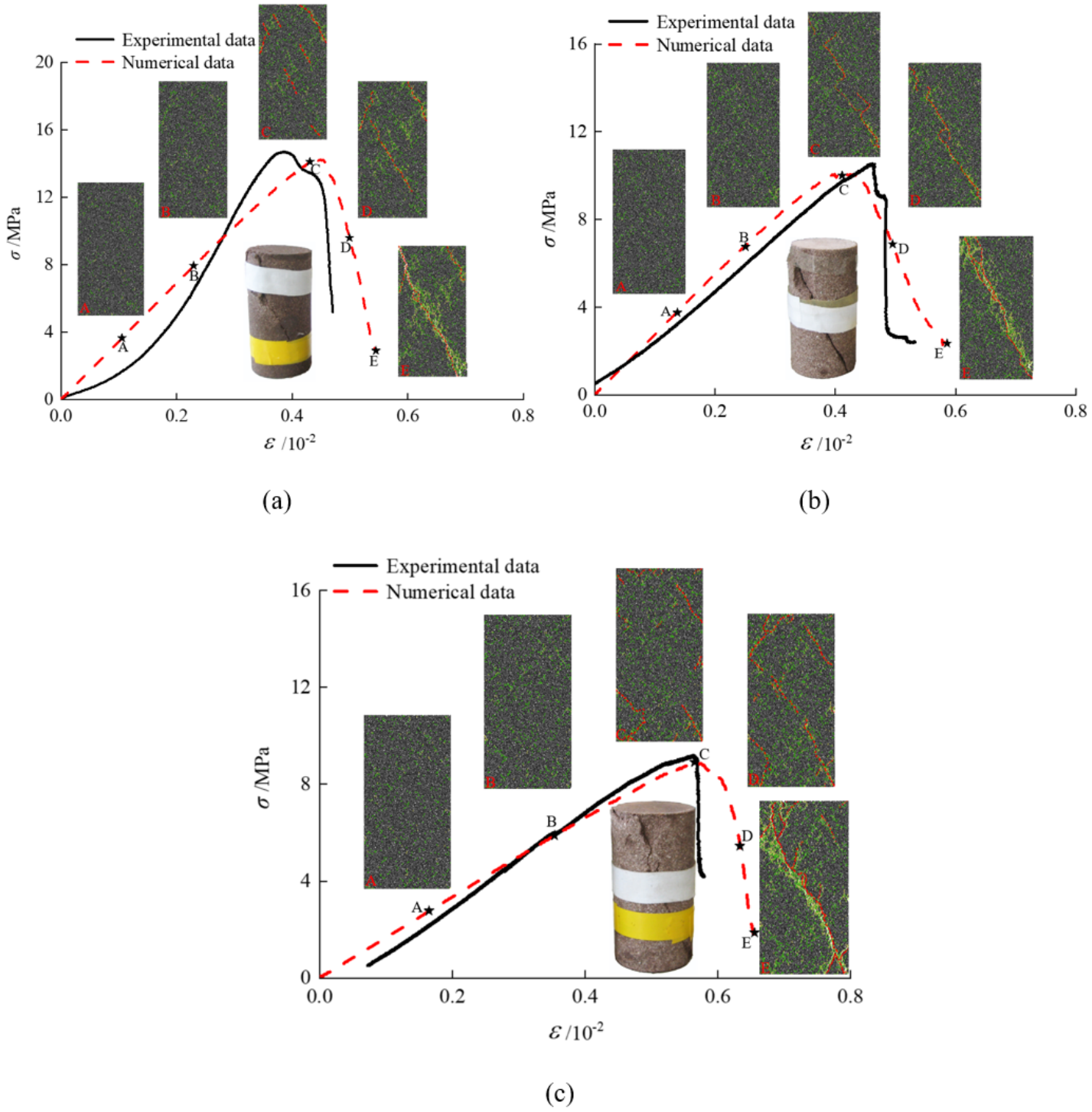

Figure 10

Stress-strain curve and crack evolution of coarse-grained sandstone; (a) coarse-grained sandstone sample 1; (b)coarse-grained sandstone sample 2; (c) coarse-grained sandstone sample 3